7320–7331 Nucleic Acids Research, 2010, Vol. 38, No. 20 Published online 7 July 2010
doi:10.1093/nar/gkq568

Modulation of thermal stability can enhance the potency of siRNA

Haripriya Addepalli[1], Meena[1], Chang G. Peng[1], Gang Wang[1], Yupeng Fan[1], Klaus Charisse[1], K. Narayanannair Jayaprakash[1], Kallanthottathil G. Rajeev[1], Rajendra K. Pandey[1], Gary Lavine[1], Ligang Zhang[1], Kerstin Jahn-Hofmann[2], Philipp Hadwiger[2], Muthiah Manoharan[1] and Martin A. Maier[1,*]

[1]Alnylam Pharmaceuticals Inc., 300 Third Street, Cambridge, MA 02142, USA and [2]Alnylam Europe AG, Fritz-Hornschuch-Str. 9, 95326 Kulmbach, Germany

Received March 10, 2010; Revised June 4, 2010; Accepted June 7, 2010

ABSTRACT

During RNA-induced silencing complex (RISC) assembly the guide (or antisense) strand has to separate from its complementary passenger (or sense) strand to generate the active RISC complex. Although this process was found to be facilitated through sense strand cleavage, there is evidence for an alternate mechanism, in which the strands are dissociated without prior cleavage. Here we show that the potency of siRNA can be improved by modulating the internal thermodynamic stability profile with chemical modifications. Using a model siRNA targeting the firefly luciferase gene with subnanomolar IC_{50}, we found that placement of thermally destabilizing modifications, such as non-canonical bases like 2,4-difluorotoluene or single base pair mismatches in the central region of the sense strand (9–12 nt), significantly improve the potency. For this particular siRNA, the strongest correlation between the decrease in thermal stability and the increase in potency was found at position 10. Controls with stabilized sugar-phosphate backbone indicate that enzymatic cleavage of the sense strand prior to strand dissociation is not required for silencing activity. Similar potency-enhancing effects were observed as this approach was applied to other functional siRNAs targeting a different site on the firefly luciferase transcript or endogenously expressed PTEN.

INTRODUCTION

It is well established that long double-stranded RNA molecules, after being processed by the RNase III-like enzyme Dicer into short interfering RNAs (siRNAs) of ~21 nt, as well as synthetic siRNAs can be loaded into the RNA-induced silencing complex (RISC) and mediate sequence-specific gene silencing (1–3). Recently, a model for the RISC-loading complex (RLC) was generated and a mechanism proposed on how nascent siRNAs and miRNAs are transferred from Dicer into AGO2 (4). Activated RISC is composed of an Argonaute protein (AGO2 in humans) and the unpaired guide strand, which provides recognition of complementary mRNA target sequences and serves as a ruler for highly site-specific cleavage of the target RNA between positions 10 and 11 of the guide strand (5–9).

Several studies have investigated the fate of the passenger strand addressing the question of when and how it is removed from the guide strand (10–12). The data suggests that the double-stranded siRNA rather than the unpaired guide strand is loaded into RISC and, under normal conditions, strand dissociation is facilitated by cleavage of the passenger strand. This cleavage was found to occur precisely between positions 10 and 11 of the guide strand or between 9 and 10 nt, counting from the 5′-end of the passenger strand. In other words, the first enzymatic cleavage reaction of the RISC generates its activated form. Kinetic analysis showed that RISC activity is rapidly generated if the passenger strand can be cleaved, whereas modifications that impair strand cleavage were also found to impair silencing activity in cell culture.

*To whom correspondence should be addressed. Tel: +1 617 551 8274; Fax: +1 617 682 4020; Email: mmaier@alnylam.com
Present address:
Philipp Hadwiger and Kerstin Jahn-Hofmann, Roche Kulmbach GmbH, Fritz-Hornschuch-Str. 9, 95326 Kulmbach, Germany.

However, there is evidence for a slower bypass mechanism, in which the passenger strand dissociates from the guide strand without prior cleavage. For instance, miRNAs were found to efficiently be loaded into Ago2 RISC without cleavage of their natural passenger strands, presumably because the multiple mismatches typical of miRNA duplexes inhibit the cleavage-assisted mechanism while accelerating the bypass mechanism (11). In addition, several other reports indicate that sense strands heavily modified at or around the putative cleavage site can be well tolerated, suggesting that highly potent effector complexes can be generated via an alternate mechanism for passenger strand removal (13,14). When the thermodynamic profiles of a relatively large set of functional and non-functional siRNAs were compared it was found that, besides terminal asymmetry of the duplex, low internal duplex stability strongly correlated with siRNA function (15).

The goal of the present study was to explore how modulation of the thermodynamic profile through incorporation of thermally destabilizing modifications, such as universal bases and mismatches, in the passenger strand affects siRNA potency. In a model siRNA directed against luciferase some of the modifications showed an up to 5-fold increase in potency. A comparison across all nucleoside modifications studied showed that, particularly at position 10 of the sense strand (complementary to position 11 of the antisense strand), the increase in potency correlated well with a decrease in thermal stability exerted by the nucleobase modifications. To determine whether this approach could be applied more broadly to enhance siRNA activity, some representative modifications were evaluated with additional siRNAs targeting either a different site on the firefly luciferase transcript or endogenously expressed PTEN (phosphatase and tensin homolog).

MATERIALS AND METHODS

Synthesis of the 5-nitroindole ribonucleoside phosphoramidite

The 5-nitroindole ribonucleoside phosphoramidite **7** was prepared as outlined in Scheme 1 and as described below.

1-O-Methyl-2,3,5-tri-O-*(2,4-dichlorobenzyl)-D-riboside (**2**)*. 1-*O*-methyl-D-riboside **1** was synthesized as described earlier (16). To a solution of **1** (13.43 g, 81.83 mmol), and 18-crown-6 (1.34 g) in dry THF (100 ml) was added powered potassium hydroxide (69 g, 1.23 mol) and stirred at room temperature for 40–60 min. 2,4-Dichlorobenzyl chloride (51 ml, 368.2 mmol) was added drop-wise and the reaction mixture was stirred at the same temperature overnight. The solids were filtered off and the filtrate was concentrated into a crude residue, which was applied to a column of silica gel and eluted with hexanes-ethyl acetate (4:1) to give pure compound **2** (48 g, 92%) as a white solid. ^{1}H-NMR ($CDCl_3$, 400 MHz): δ 7.46–7.34 (m, 5 H, ArH), 7.24–7.16 (m, 4 H, ArH), 4.99 (s, 1 H, H-1), 4.71 [doublet of doublet (dd), 2 H, J_{gem} = 12.8 Hz, OCH_2Ar], 4.63–4.61 (m, 4 H, 2 OCH_2Ar), 4.38–4.36 (m, 1 H), 4.19–4.16 (dd, 1 H), 3.98 (d, 1 H, J = 4.4 Hz), 3.75 (dd, 1 H, J = 3.6, 10.2 Hz, H-5a), 3.66 (dd, 1 H, J = 3.6, 10.4 Hz, H-5b), 3.37 (s, 3 H, OCH_3).

1-Bromo-2,3,5-tri-O-*(2,4-dichlorobenzyl)-D-ribose (**3**)*. To a cold solution of **2** (3.22 g, 5.02 mmol) in dry dichloromethane (50 ml) cooled over an ice-bath was added HOAc-HBr (5.3 ml, 30%) and stirred at 0–25°C for 3 h. The reaction mixture was concentrated *in vacuo* and the residue obtained was co-evaporated with toluene (3 × 30 ml). The crude syrupy product thus obtained could be used for the next reaction without further purification, after drying under vacuum overnight.

1-(5-Nitroindole)-2,3,5-tri-O-*(2,4-dichlorobenzyl)-D-riboside (**4**)*. Sodium hydride (602 mg, 15.06 mmol, 60%) was added to a solution of 5-nitroindole (2.44 g, 15.06 mmol) in anhydrous CH_3CN (30 ml) over an ice bath and stirred at ambient temperature for 3–4 h under argon atmosphere. The above obtained sugar donor **3** in anhydrous CH_3CN (10 ml) was added to the reaction mixture and stirred at the same temperature under argon overnight. The solids were filtered off and the filtrate was concentrated into a crude residue, which was applied to a column of silica gel and eluted with hexanes-ethyl acetate (3 : 1) to yield compound **4** (2.16 g, 60%) as mixture of α and β isomers (1:1).

*1-[5-*O-*[bis(4-methoxyphenyl)phenylmethyl]-**β**-D-ribofuranosyl]-5-nitro-1H-indole (**5a**) and 1-[5-*O-*[bis(4-methoxyphenyl)phenylmethyl]-**α**-D-ribofuranosyl]-5-nitro-1H-indole (**5b**)*. BCl_3 in dichloromethane (23 ml, 1.0 M) was added to a cold solution of **4** (1.16 g, 1.51 mmol) in anhydrous dichloromethane (100 ml) at −78°C and stirred at the same temperature for 2 h under argon and at −40°C for 2 h. The reaction mixture was quenched with methanol–dichloromethane (1:1, 50 ml) and neutralized with ammonia–methanol solution. The solids were filtered off and the filtrate was concentrated to a crude residue, which was applied to a column of silica gel and eluted with dichloromethane–methanol (10:1) to give a pure compound (300 mg, 68%) as a mixture of α and β isomers (1:1). The mixture (840 mg, 2.86 mmol) thus obtained was taken in anhydrous pyridine (3–4 ml); DMAP (90 mg) and DMT-Cl (1.06 g, 3.13 mmol) were added and stirred at ambient temperature under argon overnight. The reaction mixture was concentrated *in vacuo* and was subsequently purified by column chromatography (eluent: hexanes-ethyl acetate, 1:1) to afford the desired β isomer **5a** (550 mg, 32.3%), the corresponding α isomer **5b** (190 mg, 11.2%) and a mixture of both compounds (360 mg, 21.1%). The α isomer **5b** with the higher R_f-value eluted first followed by the mixture and single isomer **5a**.

Compound **5a**: ^{1}H-NMR ($CDCl_3$, 2D g-COSY and 2D NOESY, 400 MHz): δ 8.49 (d, 1 H, J = 1.6 Hz), 8.35 (d, 1 H), 8.03 (dd, 1 H, J = 2.0, 9.0Hz), 7.70–7.69 (m, 2 H), 7.47–7.14 (m, 8 H, ArH), 6.86–6.81 (m, 5 H, ArH), 6.71 (d, 1 H, J = 3.6 Hz), 6.41 (d, J = 5.2 Hz, H′-1), 4.73 (t, 1 H, J = 4.8Hz, H′-2), 4.46–4.42 (m, 3 H, H′-3, H′-4,

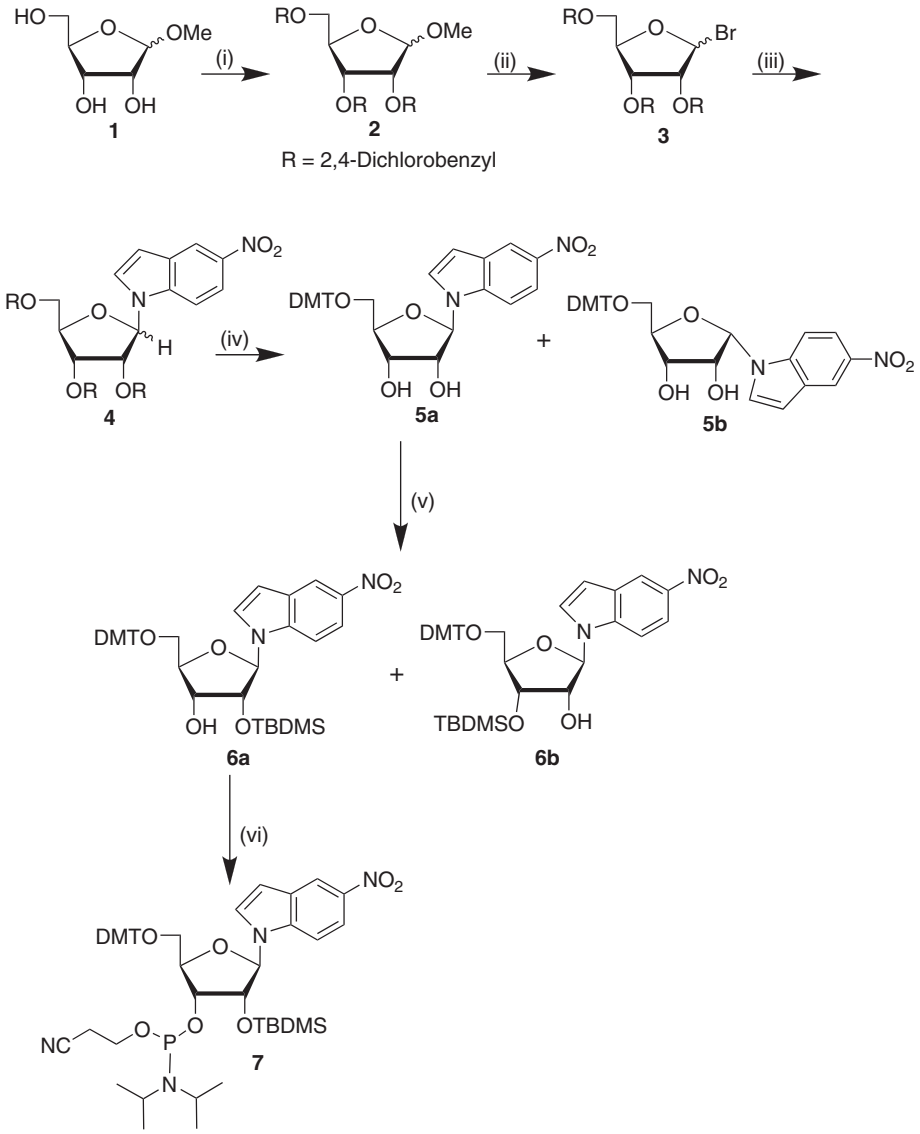

Scheme 1. Synthesis of 5-nitroindole ribonucleoside phosphoramidite. (i) KOH, 2,4-dichlorobenzyl chloride, 18-crown-6/THF, room temperature, overnight, 92%; (ii) HOAc-HBr, 0–25°C, 3 h; (iii) NaH, 5-nitroindole/MeCN, ice bath to room temperature, 4 h, Ar atm. 60%; (iv-a) BCl_3/CH_2Cl_2, −78°C for 2 h, −40°C for 2 h, α/β ratio 1:1; 68% and (iv-b). DMT-Cl, DMAP/Py, overnight, Ar. atm., combined yield: 64% (β isomer **5a** (33%), α isomer **5b** (11%) and mixture 21%); (v) TBDMS-Cl, $AgNO_3$, Py/THF, room temperature, overnight, combined yield: 75% (**6a**: 35%, **6b**: 23% and mixture: 17%); (vi) 2-cyanoethyl-*N*,*N*-diisopropylchlorophosphoramidite, DIEA/CH_2Cl_2, room temperature, overnight, 83%.

H′-5), 3.79 (s, 6 H, $2OCH_3$), 3.51 (dd, 1 H, J = 3.2, 10.4 Hz, H′-5a), 3.26 (dd, 1 H, J = 3.2, 10.6 Hz, H′-5b); MW_{calc} for $C_{34}H_{32}N_2O_8$ $(M + H)^+$: 597.22, MW_{found}: 597.23.

Compound **5b**: ^{1}H-NMR ($CDCl_3$, 2D g-COSY and 2D NOESY, 400 MHz): δ 8.55 (d, 1 H, J = 2.0Hz), 7.98 (dd, 1 H, J = 2.4, 9.2 Hz), 7.60 (d, 1 H, J = 9.2 Hz), 7.53 (d, 1 H, J = 3.2 Hz), 7.44–7.42 (m, 2 H), 7.34–7.24 (m, 7 H, ArH), 6.84–6.81 (m, 4 H, ArH), 6.68 (d, 1 H, J = 3.2 Hz), 6.00 (d, 1 H, J = 5.2 Hz, H′-1), 4.53 (t, 1 H, J = 7.6 Hz), 4.46–4.44 (m, 1 H), 4.23–4.20 (m, 1 H), 3.80–3.76 (m, 7 H, $2OCH_3$, H′-5), 3.55 (dd, 1 H, H′-5a), 3.43 (dd, 1 H, H′-5b); MW_{calc} for $C_{34}H_{32}N_2O_8$ $(M + H)^+$: 597.22, MW_{found}: 597.24.

*1-[5-*O*-[bis(4-methoxyphenyl)phenylmethyl]-2-*O*-[(1,1-dimethylethyl)dimethylsilyl]-β-D-ribofuranosyl]-5-nitro-1H-indole (**6a**) and 1-[5-*O*-[bis(4-methoxyphenyl)phenylmethyl]-3-*O*-[(1,1-dimethylethyl)dimethylsilyl]-β-D-ribofuranosyl]-5-nitro-1H-indole (**6b**)*. TBDMSCl (188 mg, 1.20 mmol) was added to a solution of **5a** (550 mg, 0.92 mmol), $AgNO_3$ (188 mg, 1.10 mmol), and pyridine (0.74 ml, 9.2 mmol) in dry THF (9.2 ml) and stirred at room temperature under an argon atmosphere overnight. The solids were filtered off and the filtrate was concentrated into a crude residue, which was applied to a column of silica gel and eluted with hexanes-ethyl acetate (4 : 1). Under the isocratic eluent condition, the faster moving compound **6a** with a slightly higher R_f-value

(0.4) was eluted first followed by mixture of **6a** and **b** and then the pure fraction of compound **6b** (R_f value: 0.35). After analyzing column fractions individually by TLC the pure fractions were pooled and evaporated *in vacuo* to obtain compounds **6a** (230 mg, 35%), **6b** (150 mg, 23%), and a mixture of compound **6a** and **b** (110 mg, 17%) in total yield of 75%. After purification, the purity of each isomer was confirmed by TLC and by NMR. The characteristic H2′ chemical shift of compound **6a** appeared as a doublet of doublet (dd) at 4.69 ppm and H3′ chemical shift was indistinguishable from H4′. The H3′ peak of isomer **6b** showed a downfield shift to 4.51 p.p.m. The identities of the two isomers were further confirmed by 2D proton NMR (g-COSY and NOESY).

Compound **6a**: ^{1}H-NMR ($CDCl_3$, 2D g-COSY, 2D NOESY, 400 MHz): δ 8.56 (d, 1 H, J = 2.4 Hz), 7.88 (dd, 1 H, J = 2.4, 8.8 Hz), 7.62 (d, 1 H, J = 9.2 Hz), 7.54 (d, 1 H, J = 3.6 Hz), 7.46–7.44 (m, 2 H), 7.36–7.25 (m, 6 H, ArH), 6.85–6.83 (d, 5 H, ArH), 6.69 (d, 1 H, J = 3.6 Hz), 5.94 (d, 1 H, J = 7.2 Hz, H′−1), 4.69 (dd, 1 H, H′−2), 4.31–4.29 (m, 2 H, H′-3, H′-4), 3.80 (s, 6 H, 2OCH_3), 3.58 (dd, 1 H, J = 2.0, 10.6 Hz, H′-5a), 3.40 (dd, 1 H, J = 2.0, 10.4 Hz, H′-5b), 2.85 (d, 1 H, J = 0.8 Hz, 3′-OH), 0.78 (s, 9 H, t-Bu), −0.016 (s, 3 H, $SiCH_3$), −0.43 (s, 3 H, $SiCH_3$); MW_{calc} for $C_{40}H_{46}N_2O_8Si$ $(M + Na)^+$: 733.29, MW_{found}: 733.30.

Compound **6b**: ^{1}H-NMR ($CDCl_3$, 2D g-COSY, 2D NOESY, 400 MHz): δ 8.61 (d, 1 H, J = 2.4 Hz), 8.05 (dd, 1 H, J = 2.0, 8.8 Hz), 7.69–7.65 (m, 2 H), 7.47–7.45 (m, 2 H, ArH), 7.36–7.27 (m, 5 H, ArH), 6.86–6.83 (m, 3 H, ArH), 6.71 (d, 1 H, J = 3.2 Hz), 5.99 (d, 1 H, J = 4.8 Hz, H′-1), 4.51 (t, 1 H, J = 4.8, 5.6 Hz, H′-3), 4.40–4.36 (m, 1 H, H′-2), 4.17–4.15 (m, 2 H, H′-4, H′-5), 3.82 (s, 3 H, OCH_3), 3.81 (s, 3 H, OCH_3), 3.63 (dd, 1 H, J = 2.4, 11.0 Hz, H′-5a), 3.31 (dd, 1 H, J = 2.8, 11.0 Hz, H′-5b), 2.95 (d, 1 H, J = 6.0 Hz, 2′-OH), 0.91 (s, 9H, t-Bu), 0.05 (s, 3 H, $SiCH_3$), 0.00 (s, 3 H, $SiCH_3$); MW_{calc} for $C_{40}H_{46}N_2O_8Si$ $(M + Na)^+$: 733.29, MW_{found}: 733.28.

*1-[5-*O*-[bis(4-methoxyphenyl)phenylmethyl]-3-*O*-[[bis(1-methylethyl)amino](2-cyanoethoxy)phosphino]-2-*O*-[(1,1-dimethylethyl)dimethylsilyl]-β-D-ribofuranosyl]-5-nitro-1H-indole (7).* 2-Cyanoethyl-*N*,*N*-diisopropylchlorophosphoramidite (900 mg, 3.80 mmol) was added to a solution of **6a** (1.0 g, 1.41 mmol) and diisopropylethylamine (1 ml, 4 eqv.) in dry dichloromethane (10 ml). The reaction mixture was stirred at ambient temperature overnight under argon atmosphere. The reaction mixture was concentrated to a crude residue, which was applied to a column of silica gel packed in hexanes containing 2% triethylamine and eluted with 10–25% ethyl acetate in hexanes to give a pure title compound **7** (1.10 g, 86%) as an amorphous solid. ^{31}P-NMR ($CDCl_3$, 400 MHz): δ 149.53 (s), 146.56 (s).

RNA synthesis

RNA oligonucleotides (Supplementary Tables S1–8) were synthesized at a scale of 1–2 μmol on a ABI 394 DNA/RNA synthesizer using commercially available 5′-*O*-DMT-3′-*O*-(2-cyanoethyl-*N*,*N*-diisopropyl) phosphoramidite monomers (ChemGenes Corporation) of uridine, 4-*N*-acetylcytidine (C^{Ac}), 6-*N*-benzoyladenosine (A^{Bz}) and 2-*N*-isobutyrylguanosine (G^{iBu}) with 2′-*O*-TBDMS protection and 5′-*O*-DMT-thymidine-3′-*O*-(2-cyanoethyl-*N*,*N*-diisopropyl) phosphoramidite (dT) following standard protocols for solid phase synthesis and deprotection (17,18). 5′-*O*-DMT-2′-deoxy-2,4--difluorotoluene-ribofuranosyl-3′-[(2-cyanoethyl)-(*N*,*N*-diisopropyl)]-phosphoramidite, 5′-*O*-DMT-2′-deoxy-5-nitroindole-ribofuranosyl-3′-[(2-cyanoethyl)-(*N*,*N*-diisopropyl)]-phosphoramidite, 5′-*O*-DMT-2′-deoxyinosine-3′-[(2-cyanoethyl)-(*N*,*N*-diisopropyl)]-phosphoramidite, 5′-*O*-DMT-inosine-2′-*O*-TBDMS-3′-[(2-cyanoethyl)-(*N*,*N*-diisopropyl)]-phosphoramidite, 5′-*O*-DMT-2′-deoxynebularine-3′-[(2-cyanoethyl)-(*N*,*N*-diisopropyl)]-phosphoramidite, 5′-*O*-DMT-nebularine-2′-*O*-TBDMS-3′-[(2-cyanoethyl)-(*N*,*N*-diisopropyl)]-phosphoramidite, and 2-(*O*-DMT-oxymethyl)tetrahydrofurane-3-[(2-cyanoethyl)-(*N*,*N*-diisopropyl)]-phosphoramidite (dSpacer) were obtained from Glen Research and used according to the manufacturer's protocols. 5′-*O*-DMT-2-*N*-(dimethylaminomethylidene)-2′-deoxy-2-aminopurine ribofuranosyl-3′-[(2-cyanoethyl)-(*N*,*N*-diisopropyl)]-phosphoramidite and 5′-*O*-DMT-2-*N*-isobutyryl-2-aminopurine ribofuranosyl-2′-*O*-TBDMS-3′-[(2-cyanoethyl)-(*N*,*N*-diisopropyl)]-phosphoramidite were obtained from ChemGenes Corporation. We reported earlier on the synthesis of 5′-*O*-DMT-2,4-difluorotoluene-2′-*O*-TBDMS-ribofuranosyl-3′-[(2-cyanoethyl)-(*N*,*N*-diisopropyl)]-phosphoramidite (19).

The crude oligonucleotides were analyzed by LC–MS and purified by anion-exchange high-performance liquid chromatography (IEX-HPLC) with TSK-Gel Super Q-5PW support (TOSOH Bioscience, Inc.) using a linear gradient of 22–42% buffer B in 130 min. Solutions of 0.02 M Na_2HPO_4 in 10% CH_3CN, pH 8.5 and 0.02 M Na_2HPO_4/1 M NaBr in 10% CH_3CN pH 8.5 were used as eluents A and B, respectively. To ensure high fidelity of the data, all single strands were HPLC purified to >85% purity and purified oligonucleotides were desalted by size exclusion chromatography on an Aekta Prime chromatography system using an AP-2 glass column (Waters Corporation) packed with Sephadex G25 (GE Healthcare). The purity and identity of the oligonucleotides was confirmed by ion exchange chromatography and LC–MS, respectively.

Duplex annealing

For duplex annealing, 1 mM stock solutions in de-ionized water were prepared for all single strands used in this study. For the cell culture experiments, 0.05 mM stock solutions of siRNA in PBS were prepared by mixing equimolar amounts of complementary sense and antisense strands in PBS buffer and heating the solution to 95°C for 10 min and allowing it to slowly cool to room temperature to complete the annealing process. To ensure low variability in duplex concentration, the optical densities of the final duplex solutions in PBS buffer were measured and the duplex preparation was repeated if the optical density

was not within a 10% range of a reference sample (parent duplex).

Thermal melting experiments

Experiments to determine the melting temperature (T_m) of siRNAs were performed with siRNA samples in sterile 0.9% physiological saline solution (154 mM sodium chloride in water for injection, pH 6.8). Prior to melting experiments, siRNA duplexes were heated to 95°C for ~5 min in a water bath, and then slowly cooled off in the same water bath until they reached temperature below 35°C. The sample concentration was adjusted to ~0.4 OD/ml by diluting the sample appropriately with physiological saline solution. Samples were then filtered through a 0.45 µm nylon filter (Whatman) into a 1 cm optical path length dry quartz micro-cuvette. The cuvettes where capped with a Teflon cap and absorbance values at 260 nm were collected over the range 25–95°C using a Beckman Coulter DU800 UV/VIS instrument with T_m extension. Samples were allowed to equilibrate for 5 min at the beginning temperature of each heating-cooling cycle. Temperature was increased linearly at a rate of ~0.5°C/min while the absorbance was monitored continuously. At the beginning of the measurement baseline adjustment was carried out against the 0.9% physiological saline solution. The T_m values were calculated by the Beckman Coulter DU800 UV/VIS software. All experiments were run in duplicate with less than ±0.1°C T_m value difference between runs.

Cell culture

Tissue culture medium, trypsin and Lipofectamine 2000 were purchased from Invitrogen. HeLa cells were obtained from the American Type Tissue Collection. The luciferase plasmids, renilla luciferase (pRL-CMV), firefly luciferase (pGL3) and the Dual Glo Luciferase Assay kit were purchased from Promega. HeLa SS6 cells, stably transfected with the luciferase plasmids, renilla luciferase (pRL-CMV) and firefly luciferase (pGL3), were grown at 37°C, 5% CO_2 in Dulbecco's modified Eagles's medium (GIBCO, Invitrogen) supplemented with 10% fetal bovine serum and 0.5 mg/ml zeocin and 0.5 µg/ml puromycin (selective for cells transfected with plasmids). The cells were maintained in exponential growth phase.

Luciferase assay

The cells were plated in 96-well plates (0.1 ml medium per well) to reach ~90% confluence at transfection. The cells were grown for 24 h and the culture medium was changed to OPTIMEM 1 (GIBCO, Invitrogen), 0.5 ml per well. Transfection of siRNAs was carried out with Lipofectamine 2000 (Invitrogen) as described by the manufacturer for adherent cell lines in the siRNA concentration range of 0.002–8.0 nM. The final volume was 150 µl per well. The cells were harvested 24 h after transfection, and lysed using passive lysis buffer (PLB), 100 µl per well, according to the instructions of the Dual-Luciferase Reporter Assay System (Promega). The luciferase activities of the samples were measured using a Victor FL Luminometer (Perkin Elmer Corporation). The volumes used were: 20 µl of sample and 75 µl of each reagent (luciferase assay reagent II and Stop and Glo Reagent). The inhibitory effects generated by siRNAs were expressed as normalized ratios between the activities of the reporter (firefly) luciferase gene and the control (renilla) luciferase gene relative to untreated controls (no siRNA, but with Lipofectamine 2000). Values represent the mean of triplicates. The potency of the siRNAs was determined by calculating the IC_{50}-values from the corresponding dose-response curves using XL-Fit software.

PTEN assay

The cells were plated in 96-well plates (0.1 ml medium per well) to reach ~90% confluence at transfection. The cells were grown for 24 h and the culture medium was changed to OPTIMEM 1 (GIBCO, Invitrogen), 0.5 ml per well. Transfection of siRNAs was carried out with Lipofectamine 2000 (Invitrogen) as described by the manufacturer for adherent cell lines in the siRNA concentration range of 0.002–8.0 nM. Post-transfection, the cells were lysed using Lysis Mixture (Panomics Quantigene Assay Kit) and lysates were transferred to a 96-well plate in the presence of PTEN specific probe sets (Panomics Quantigene Assay Kit) and then incubated at 53°C overnight. On Day 2, the wells were washed and then incubated with amplifier (Panomics Quantigene Assay Kit) at 46°C for 60 min, followed by three washes and then incubated with label probe for 60 min at 46°C. After the final wash, chemoluminescent substrate (Panomics Quantigene Assay Kit) was added to each well and incubated for 30 min at 46°C followed by quantification of the signal by a Victor FL Luminometer (Perkin Elmer Corporation). Results were normalized to housekeeping gene (GAPDH) signals for mRNA expression across samples. Values represent the mean of triplicates. Additionally, a control, excluding cell lysate, was used to determine any possible background signal from reagents.

RESULTS

Effect of mismatches

The simplest way to locally destabilize siRNA duplexes is to introduce base pair mismatches at the desired position. Dependent on the mismatched base pair, its position in the duplex, and the sequence, the thermal stability of a duplex, as measured by the melting temperature in thermal denaturation experiments (T_m), can decrease over a wide range, typically between 1 and 12 K compared to the fully complementary duplex (Supplementary Table S1). Based on the parent unmodified RNA/RNA duplex of siRNA-1 targeting firefly luciferase, all possible mismatch combinations were walked through the entire sequence of the sense strand, while the antisense strand was left unchanged and hence fully complementary to the target sequence on the mRNA.

Comparing the terminal mismatches, it appears that destabilizing the 5′-end of the sense strand (position 1) led to a decrease in activity, while for incorporation of

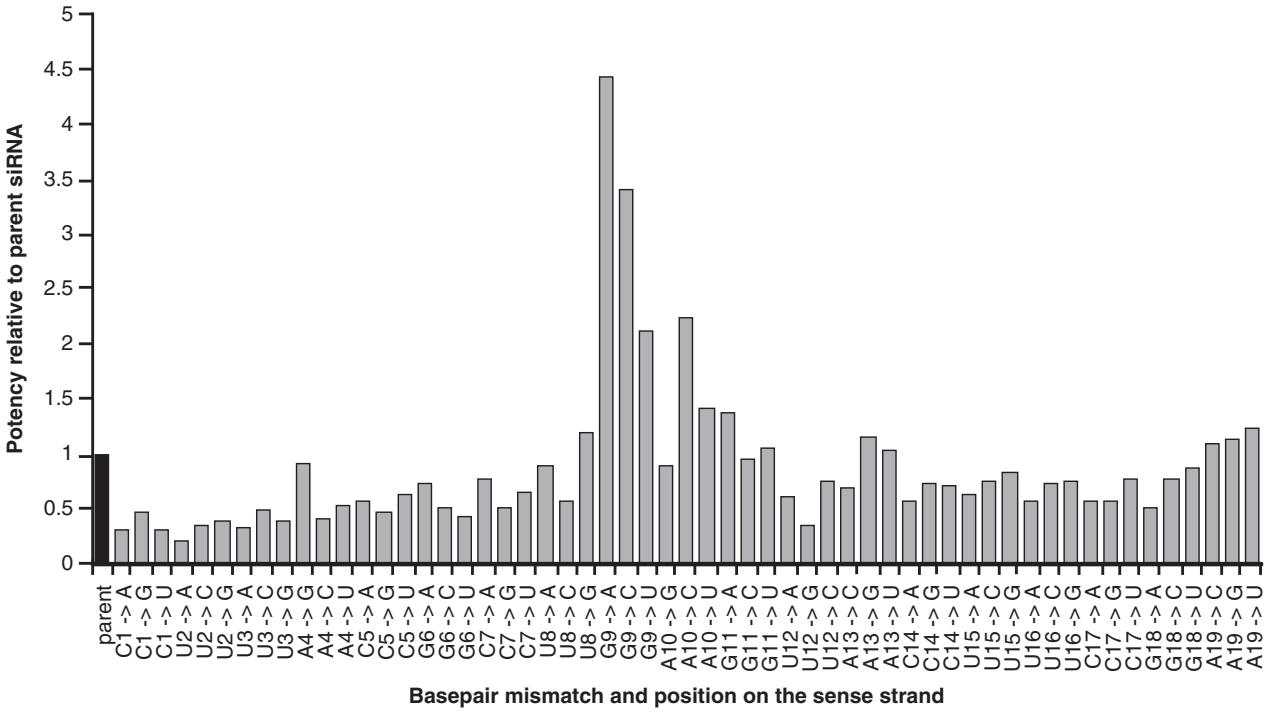

Figure 1. Effect of base pair mismatches across the sense strand sequence of siRNA-1 on potency relative to the parent duplex plotted as IC_{50} (parent)/IC_{50} (modified).

base pair mismatches at the 3′-end (position 19) no changes in potency were observed (Figure 1). This is in good agreement with the selection of guide and passenger strand based on thermal asymmetry in the siRNA duplex (15,20) and indicates that the model siRNA used in this work was sufficiently biased for loading of the antisense strand. Interestingly, some siRNAs with mismatches in the central region, particularly at positions 9 and 10, exhibited an increase in potency, as measured by a decrease in the IC_{50}-values and expressed as the ratio of IC_{50} (parent) to IC_{50} (modified). In contrast, most mismatches at the other internal positions (2–8 and 12–18) showed the opposite trend.

Effect of base modifications in the central region of the passenger strand

Non-polar nucleobase analogs, such as 2,4-difluorotoluene (F), an isostere of thymine or 5-nitroindole, a purine analog, destabilize nucleic acid duplexes predominantly because they have no or very limited capability to form hydrogen bonds with the nucleobase in the opposite strand (21–23). In one example, crystal structure studies of duplexes containing F indicate the presence of unconventional hydrogen bonds in F:G pairs [F and H–N1(G)]. The corresponding duplexes show a deviation from the canonical backbone shape (24). When placed in the antisense strand of siRNA, the effect of F residues on silencing activity was found to be dependent on both, the position in the sequence and the residue replaced with F:G pairs much less tolerated than F:A (19,25).

Based on the findings with the mismatched base pairs, we focused our efforts on the central region (positions 9–12) of the sense strand and replaced single nucleotides with various nucleobase modifications, both as ribo- as well as deoxyribofuranosyl nucleotides (Figure 2). In addition to the hydrophobic nucleobase isosteres 2,4-difluorotoluene (F) and 5-nitroindole (N), other nucleobase analogs, such as inosine (I), nebularine (Neb) and 2-aminopurine (2AP), which are capable of forming hydrogen bonds with natural bases, were investigated.

Similar to the base pair mismatches, the degree of thermal destabilization of the duplex varied between 1 and 12 K compared to the unmodified parent compound (Supplementary Table S2). The effect of the modifications on the potency of the siRNA were found to be dependent on the position as well as the type of nucleobase modification used (Figure 3A and B and Supplementary Figure S1). The non-polar isostere F exhibited a greater and more position-dependent effect than any of the other nucleobase analogs. In contrast, placement of N, which had previously been shown to be the most 'universal' base (23), was found to be relatively position-independent. Comparing the ribo- and deoxyribofuranosyl analogs, there appears to be no obvious correlation between the structure of the pentose (ribose or deoxyribose) and the observed effects.

Correlation of potency enhancement with decrease in thermal stability

The *in vitro* silencing data shows that, in general, destabilizing modifications in the central region of the

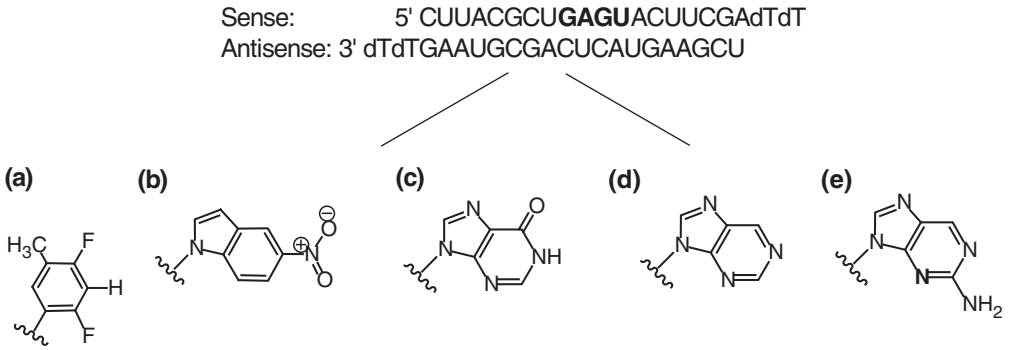

Figure 2. Base modifications in the central region of the sense strand of siRNA-1: the positions of the parent duplex, which were replaced against the nucleotide analogs, are shown in bold. (**a**) 2,4-difluorotoluene (F and dF); (**b**) 5-nitroindole (N and dN); (**c**) inosine (I and dI); (**d**) nebularine (Neb and dNeb); (**e**) 2-aminopurine (2AP and d2AP).

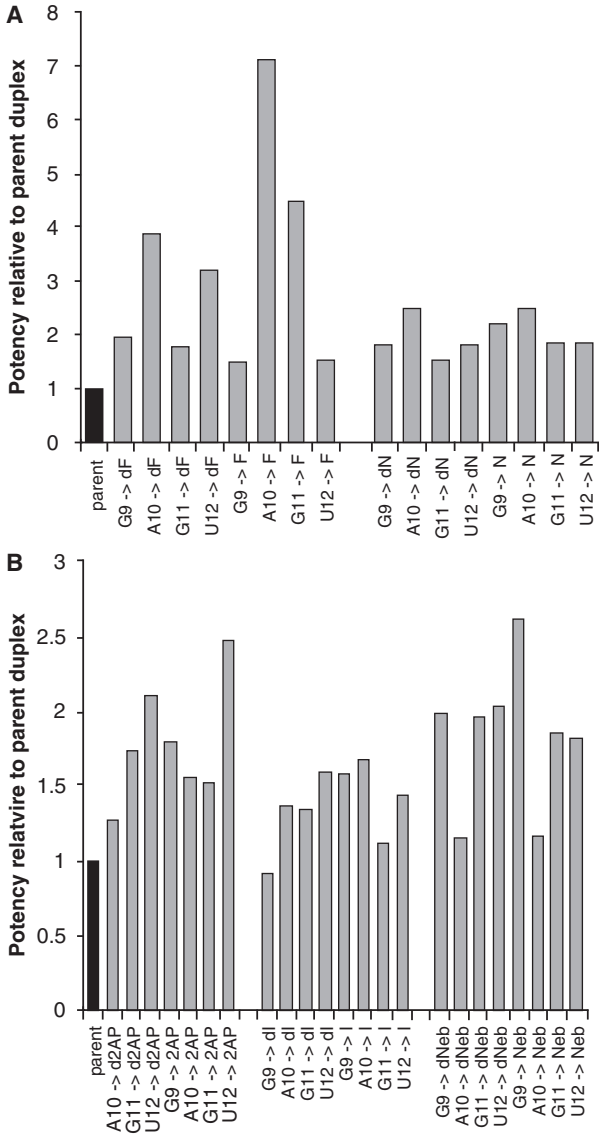

Figure 3. Effect of nucleobase modifications in positions 9–12 of the sense strand of siRNA-1: (**A**) ribo- and deoxyribo versions of non-polar nucleobase isosteres 2,4 difluorotoluene (F, dF) and 5-nitroindole (N, dN); (**B**) ribo- and deoxyribo versions of the nucleobase analogs 2-aminopurine (2AP, d2AP), inosine (I, dI) and nebularine (Neb, dNeb); changes in potency relative to the parent siRNA are expressed as IC_{50} (parent)/IC_{50} (modified).

sense strand are not only well tolerated and but can even be potency enhancing. The magnitude of the effect, however, appears to be quite variable and seems to depend on the modification as well as its position. Obviously, all nucleobase and mismatch modifications introduced in this region affect the thermal stability of the siRNA duplexes. However, dependent on the nature of the non-canonical base pair formed between the modified base in the sense strand and its counterpart in the antisense strand, the degree of destabilization can be expected to vary significantly.

Focusing on the central positions 9–12, the thermal denaturation T_m of each duplex was determined (Supplementary Table S2) and the correlation between thermal stability and activity was investigated. Figure 4 shows the fold decrease in IC_{50} as a function of ΔT_m between the parent and the modified duplex. While at positions 9, 11 and 12 the effect of the modifications on the IC_{50} appears to be more or less independent of the extend of thermal destabilization, a strong correlation with a R^2 value of 0.76 was observed only at position 10.

Head-to-head comparison of selected modifications

To confirm the previous results and to determine the variability between separate experiments, a selected set of modified siRNAs, including some of the most potent ones, were subjected to a head-to-head comparison in three independent transfection experiments. Figure 5 shows the dose–response curves of a representative experiment and potency enhancement of the modified siRNAs relative to the parent compound averaged over three independent experiments.

Although there is, as can be expected, some variability, the rank order by IC_{50} across the independent experiments is very similar (Supplementary Table S3) and the data shows that the non-polar nucleobase isosteres 2,4-difluorotoluene and 5-nitroindole, when incorporated at position 10, led to a significant increase in potency. The effect was less pronounced with nucleobase analogs, which are capable of forming hydrogen bonds with natural bases, such as I and Neb. Particularly at position 10, these modifications were found to have a smaller impact

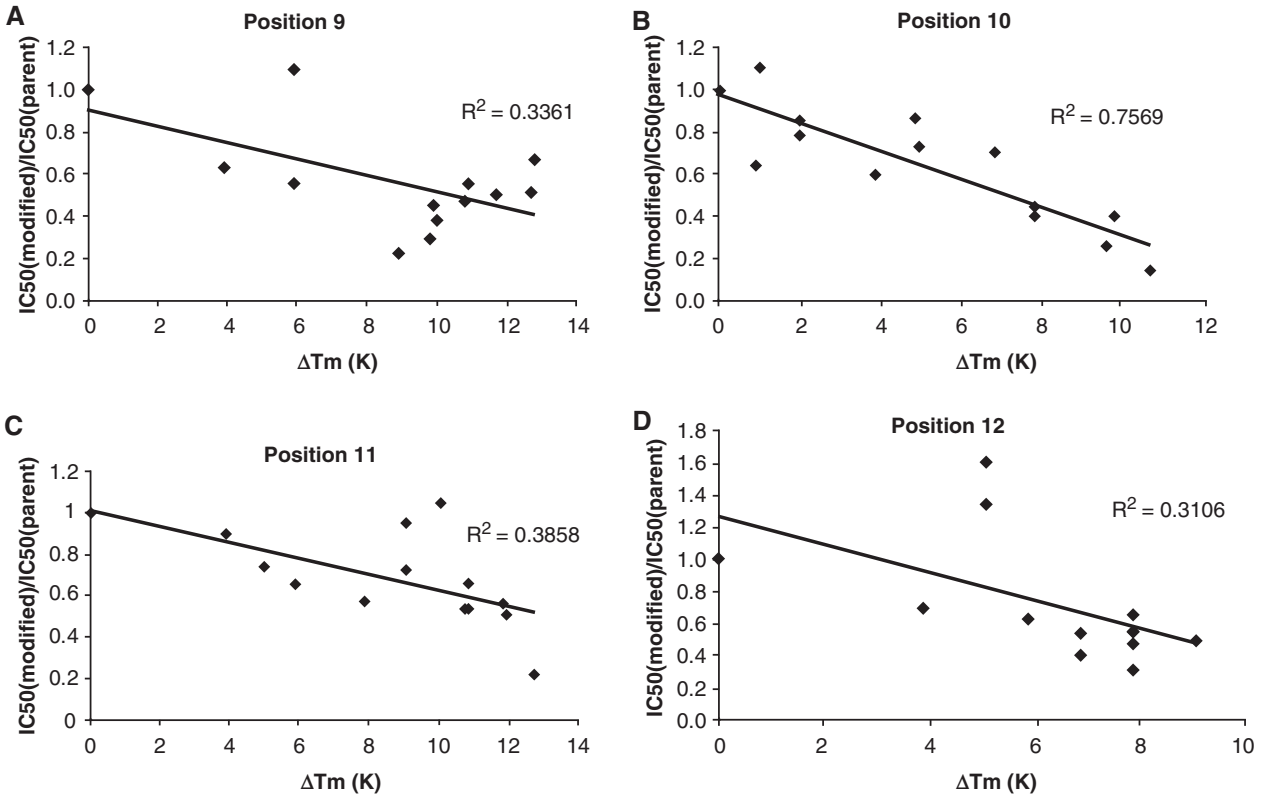

Figure 4. Correlation between the decrease in IC_{50} and the thermal destabilization of the modified siRNAs compared to the parent unmodified siRNA-1 calculated as $\Delta T_m = T_m(\text{parent}) - T_m(\text{modified})$. Modifications were incorporated in (**A**) position 9, (**B**) position 10, (**C**) position 11 and (**D**) position 12.

on thermal stability compared to 2,4-difluorotoluene and 5-nitroindole (Supplementary Table S2).

Effect of backbone modifications

As shown above, the presence of mismatches or nucleobase analogs adjacent to the putative cleavage site on the sense strand between 9 and 10 nt generally leads to enhanced silencing activity although those modifications can be expected to decrease the rate of enzymatic cleavage or even prevent it. On the other hand, in a previously reported study it was observed that the activity of a luciferase siRNA was impaired after introducing backbone modifications, such as 2′-*O*-methyl-modification at position 9 and/or a phosphorothioate linkage between nucleotides 9 and 10, into the sense strand (10). It targets the same site on the luciferase transcript as siRNA-1 used in the present work but contains 3′-overhangs of different sequence and chemistry. To rule out any involvement of sense strand cleavage and to confirm that the observed potency enhancement is solely due to thermal destabilization of the central part of the duplex, two additional experiments were performed: (i) each of the 9–12 nt in the central region of the sense strand were replaced by an abasic modification, 2-hydroxymethyl-tetrahydrofurane-3-ol; (ii) the putative cleavage site in the sense strand was stabilized against enzymatic attack by incorporating a 2′-*O*-methyl-modification at position 9 and/or a phosphorothioate linkage between nucleotides 9 and 10 in both, siRNA-1 as well as siRNA-2, identical to the one described by Leuschner *et al.* (10).

Incorporation of the abasic modification was found to increase potency by ~2–3-fold compared to the parent unmodified duplex consistently across all central positions (Figure 6A). Depending on the nucleotide replaced, a decrease in thermal stability in the range of 9–15 K was observed (Supplementary Table S4). As expected, replacement of G9 or G11 yielded a larger T_m decrease compared to A10 and U12.

When the sugar-phosphate linkages at the putative cleavage site between positions 9 and 10 in the sense strands of siRNA-1 and siRNA-2 were modified with 2′-*O*-methyl or a phosphorothioate linkage, no significant effect on potency could be detected (Figure 6B and Supplementary Table S5). Even the combination of both modifications did not result in a decrease in activity. Furthermore, combined with the potency-enhancing F residue in position 10, the activity of the backbone-modified siRNAs was found to be still ~3-fold higher compared to the parent unmodified compound, albeit slightly reduced compared to the analog lacking the backbone modifications.

Additional siRNAs

To investigate whether manipulation of the thermal duplex stability could be applied more generally to enhance the potency of other functional siRNAs, a

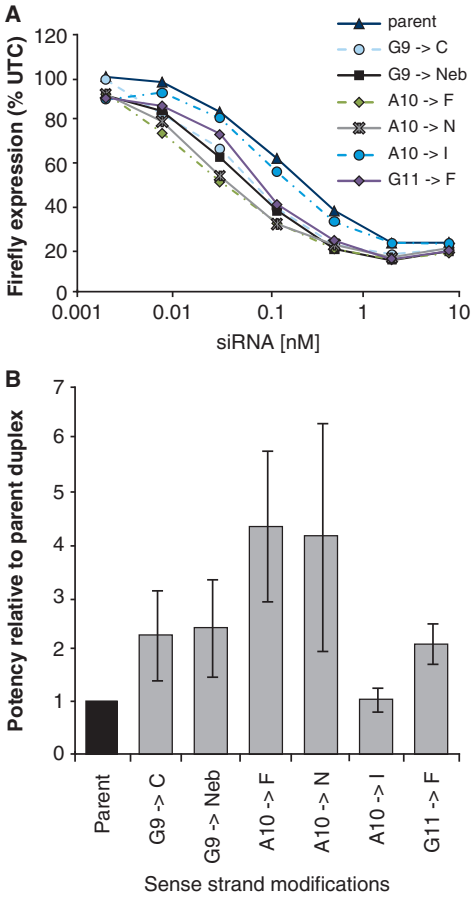

Figure 5. Head-to-head comparison of a selected set of thermally destabilizing modifications in the sense strand of siRNA-1: (**A**) representative example of dose-dependent silencing of firefly luciferase as percent untreated control; (**B**) potency enhancement of the modified siRNAs relative to the parent duplex (average of three independent transfection experiments).

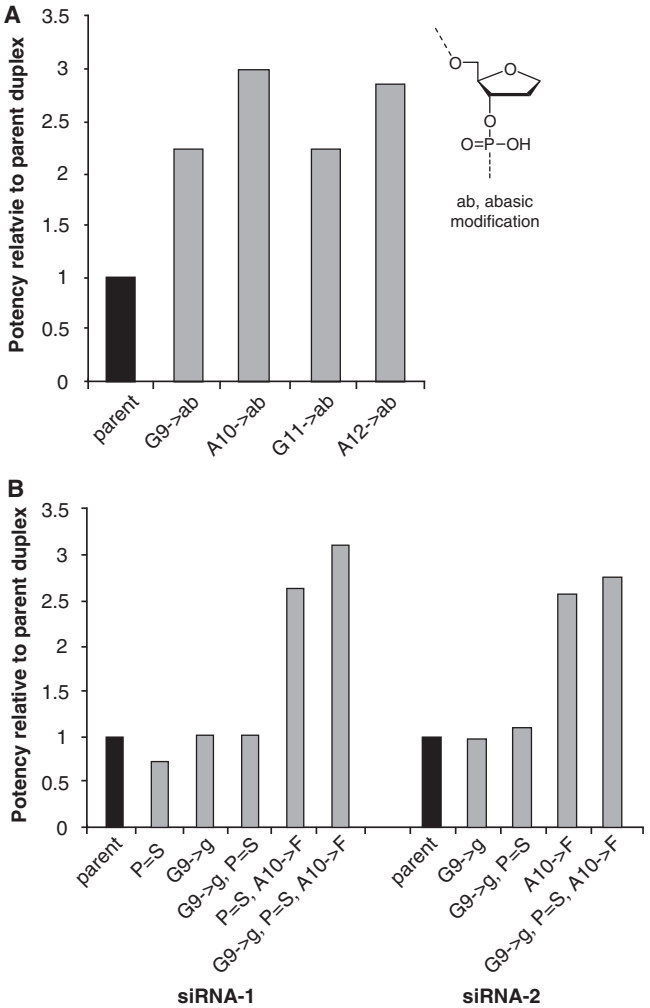

Figure 6. (**A**) Effect of abasic modifications in positions 9–12 of the sense strand of siRNA-1; (**B**) effect of 2′-*O*-methyl and/or phosphorothioate modifications between positions 9 and 10 of the sense strands of siRNA-1 and siRNA-2; changes in potency relative to the parent siRNA are expressed as IC_{50} (parent)/IC_{50} (modified); P = S, phosphorothioate linkage between positions 9 and 10; g, 2′-*O*-methylguanosine.

selected set of thermally destabilizing modifications was introduced into the central region of the sense strands of two additional siRNAs, one targeting firefly luciferase at a different site on the transcript (siRNA-3) and one (siRNA-4) targeting endogenously expressed PTEN (13).

The nucleobase isostere 2,4-difluorotoluene (F), which had been found to yield the most pronounced potency enhancement, was walked through the central region of the sense strand of siRNA-3, an example of a chemically modified duplex containing 2′-*O*-methyl modifications at all pyrimidine positions in the sense strand as well as a few 2′-*O*-methyl modifications in the antisense strand. Both strands contain a phosphorothioate linkage in the overhangs (dTsdT). Similar to the results obtained with siRNA-1, a significant potency increase was observed when F was placed at positions 10 and 11 (Supplementary Table S6 and Figure S2).

Again focusing our efforts on the central region of the sense strand, all possible base pair mismatches at positions 9 and 10 and 2,4-difluorotoluene (F) at positions 9–12 were evaluated for siRNA-4 targeting PTEN (Supplementary Table S7). The study was carried out in three independent experiments to evaluate the reproducibility of the results (Figure 7). Replacement of C10 against A and A9 against F yielded in average an increase in potency of more than 8- and 5-fold, respectively, which correlated with a substantial decrease in T_m of ~10–11 K (Supplementary Table S7). While the other mismatches generally exhibited a smaller decrease in T_m, the effect of 2,4-difluorotoluene was relatively position-independent with a T_m-decrease in the range of 11–13 K. More data from a larger set of analogs would be required, however, to correlate potency enhancement with the decrease in thermal stability at each of the positions.

DISCUSSION

During RISC assembly, one of the strands of the siRNA, the passenger strand, has to be removed to enable the formation of the active RISC complex. Previous studies have shown that this can occur either by cleavage of the passenger strand after loading of the entire duplex into

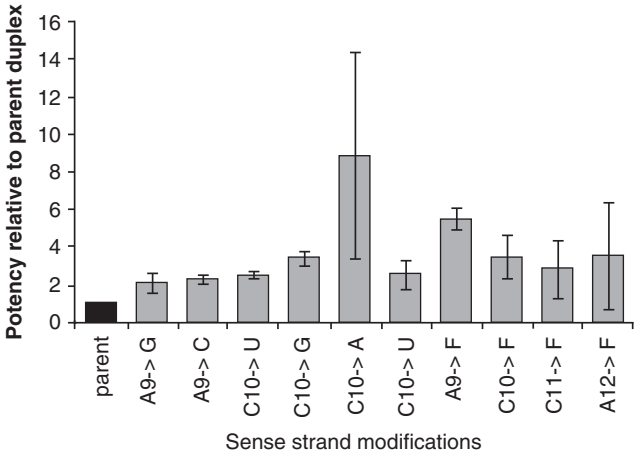

Figure 7. Effect of base pair mismatches in positions 9,10 and 2,4-difluorotoluene (F) in positions 9–12 of the sense strand of siRNA-4 targeting PTEN; changes in potency relative to the parent siRNA are expressed as IC_{50} (parent)/IC_{50} (modified).

RISC or by an alternative by-pass mechanism (10,11). The goal of the present work was to investigate whether the potency of siRNA can be further improved by modulating the thermodynamic profile with thermally destabilizing modifications, such as base pair mismatches or nucleobase analogs.

For a model siRNA targeting firefly luciferase, all possible mismatch combinations were walked through the entire duplex region of the sense strand of this siRNA composed of 19 base pairs with 3′-dTdT overhangs. In agreement with previous studies demonstrating the significance of thermodynamic asymmetry within siRNA duplexes and the concomitant bias in RISC loading (15,20), we found that mismatches at the 3′-end of the sense strand were well tolerated, while mismatches at or near the 5′-terminus significantly decreased siRNA potency. The fact that the former did not lead to further improvement in potency suggests that the parent duplex was sufficiently strand-biased for preferential loading of the antisense strand. Most mismatches within the internal sequence led to a more or less pronounced decrease in activity. Surprisingly, however, mismatches in the central region of the sense strand were not only well tolerated but, in some cases, even led to a significant increase in activity. The largest potency enhancements were found at positions 9 and 10, which frame the putative cleavage site in the sense strand.

To further investigate this phenomenon, we synthesized a variety of siRNAs bearing nucleobase analogs in one of the central positions 9–12 of the sense strand and determined their ability to silence luciferase in comparison to the unmodified parent duplex. The most pronounced potency enhancement was observed by placing the hydrophobic thymidine isostere 2,4-difluorotoluene in position 10. Other nucleobase modifications also showed some potency-enhancing effect at various positions, albeit to a lesser degree.

When a selected set of modified siRNAs, including some of the most potent ones, was re-screened, the non-polar nucleobase isosteres F and NI, incorporated at position 10, consistently showed the most pronounced increase in potency. The parent siRNA contains an adenosine residue at this position 10 and the resulting non-canonical F:U and N:U base pairs mimic the shape of a T:U and a R(purine):U base pair, respectively. Therefore, the local helix geometry can be expected to vary significantly. We have previously shown that, whether or not single F or basepair mismatches in the guide strand can be tolerated at or adjacent to the target cleavage site (positions 10 and 11), critically depends on the resulting non-canonical base pair formed (19). Subsequent studies found that the observed activities were inversely correlated with the backbone distortion resulting from the modified base pair rather than being affected by differences in thermal stability (24). If sense strand cleavage by Ago2 slicer were a critical step in the assembly of the RISC complex, one would expect to observe a strong dependence of the siRNA activity on the resulting non-canonical base pair with a clear trend towards reduced potency. However, with the siRNA used in this work, most base pair mismatches and modified bases introduced in the central region of the sense strand were not only well tolerated but even led to enhanced potency.

If cleavage of the sense strand during RISC assembly is not required, the observed increase in activity could either be due to improved interaction of the modified siRNAs with the RISC-loading complex or facilitated passenger strand removal during RISC assembly due to a decrease in thermal stability. In fact, a strong correlation between ΔT_m and potency enhancement was found at position 10, at which we also observed the most pronounced increase in activity. Although the correlation at the other positions was less significant, the most active siRNAs all exhibited a substantial decrease in T_m compared to the parent duplex.

Notwithstanding the mismatch results, the observed effects could potentially be explained by a simple increase in strand bias and preferential loading of the antisense strand due to the presence of non-natural nucleobases in the sense strand. To rule out this possibility, we investigated the effect of chemically inactivated sense and antisense strands by introducing several 2′-*O*-methoxyethyl modifications near the 5′-end (Supplementary Table S8 and Figure S3). The activity of the siRNA was virtually unchanged with the modified sense strand, while the same modifications in the antisense strand completely abolished activity. This confirms that (i) placement of a few 2′-*O*-methoxyethyl modifications at or near the 5′-end leads to strand inactivation and (ii) when placed in the sense strand, they do not improve the activity indicating that the parent siRNA is already sufficiently strand biased towards preferential loading of the antisense strand.

If the observed effect is due to thermal destabilization of the central region of the duplex, the activity should also be enhanced by other thermally destabilizing modifications incapable of interacting with the bases of the opposite strand. On the other hand, if passenger strand cleavage is not required, the activity should not be affected by backbone modifications, which stabilize against

nucleolytic cleavage. Hence, two additional sets of compounds were made and tested—one with the central nucleotides of the sense strand replaced by an abasic modification and one with modifications in the sugar-phosphate backbone at position 9. For the latter experiment, we included a siRNA, which contains different overhangs but targets the same site on the firefly luciferase transcript and which was reported previously to show impaired activity if its passenger strand is modified at or adjacent to the putative cleavage site (10). The abasic modification, which lacks the capability to form hydrogen bonds with nucleotides in the opposite strand as well as the stacking interactions with the neighboring bases, caused a large thermal destabilization of the duplex. All siRNAs modified with abasic residues not only exhibited the expected decrease in T_m but also a 2–3-fold increase in potency. In our hands and very consistent across the two siRNAs, the backbone modifications, when introduced at the putative cleavage site between positions 9 and 10 of the sense strand, did not significantly alter siRNA activity. Furthermore, siRNAs bearing F in position 10 combined with backbone modifications, still exhibited a 2–3-fold potency enhancement over to the unmodified parent duplexes. Taken together, the results indicate that, at least for the siRNAs used in this study, sense strand cleavage during RISC assembly is not a critical or rate limiting step and confirm that thermal destabilization rather than strand cleavage is responsible for the observed potency enhancement.

Since the thermodynamic profile depends on the sequence of the siRNA duplex, it can be expected that the effect of modifications, which modulate the thermal stability, is similarly dependent on sequence and position. Two additional siRNAs, one targeting firefly at a different site on the transcript and one targeting endogenously expressed PTEN, were used to determine whether this approach could be applied more broadly to enhance siRNA potency. A selected set of thermally destabilizing modifications was introduced into the central region of the sense strands of both siRNAs. Although the degree and position-dependence of the effects were found to vary slightly, the overall trend towards improved potency was confirmed. Thus, in agreement with previous reports investigating the thermodynamic profile of functional siRNAs (15), our findings suggest that the potency of a given siRNA duplex can be further improved by modulating its internal stability profile.

CONCLUSION

We investigated the effect of non-canonical base pairs and the concomitant local perturbation of the helical structure and modulation of thermal stability on siRNA potency. Our findings demonstrate that local destabilization of the central region of the duplex through placement of base pair mismatches or nucleobase modifications in the sense strand of a siRNA directed against luciferase can lead to a significant improvement in silencing activity. A comparison across all nucleoside modifications tested showed that the potency increase correlated well with a decrease in thermal stability. This trend was most pronounced at position 10 of the passenger strand. Backbone modifications at the putative sense strand cleavage site (positions 9 and 10), which are known to stabilize against enzymatic cleavage did not significantly reduce the potency-enhancing effect. When this approach was applied to other functional siRNAs targeting either a different site on the same transcript or the transcript of a different, endogenously expressed gene (PTEN), similar potency-enhancing effects were observed. In summary, our work indicates that through selective manipulation of the thermodynamic profile, and specifically by decreasing thermal stability in the central region of the duplex, the potency of a given siRNA may be further enhanced.

SUPPLEMENTARY DATA

Supplementary Data are available at NAR Online.

ACKNOWLEDGEMENTS

The authors thank Christopher Sherrill, Nathan Taneja, Jonathan O'Shea and Elena Bulgakova for technical support and Lauren Lesser for assistance in manuscript preparation.

FUNDING

Funding for open access charge: Alnylam Pharmaceuticals.

Conflict of interest statement. None declared.

REFERENCES

1. Bernstein,E., Caudy,A.A., Hammond,S.M. and Hannon,G.J. (2001) Role for a bidentate ribonuclease in the initiation step of RNA interference. *Nature*, **409**, 363–366.
2. Elbashir,S.M., Harborth,J., Lendeckel,W., Yalcin,A., Weber,K. and Tuschl,T. (2001) Duplexes of 21-nucleotide RNAs mediate RNA interference in cultured mammalian cells. *Nature*, **411**, 494–498.
3. Knight,S.W. and Bass,B.L. (2001) A role for the RNase III enzyme DCR-1 in RNA interference and germ line development in Caenorhabditis elegans. *Science*, **293**, 2269–2271.
4. Wang,H.W., Noland,C., Siridechadilok,B., Taylor,D.W., Ma,E., Felderer,K., Doudna,J.A. and Nogales,E. (2009) Structural insights into RNA processing by the human RISC-loading complex. *Nat. Struct. Mol. Biol.*, **16**, 1148–1153.
5. Liu,J., Carmell,M.A., Rivas,F.V., Marsden,C.G., Thomson,J.M., Song,J.J., Hammond,S.M., Joshua-Tor,L. and Hannon,G.J. (2004) Argonaute2 Is the Catalytic Engine of Mammalian RNAi. *Science*, **305**, 1437–1441.
6. Meister,G., Landthaler,M., Patkaniowska,A., Dorsett,Y., Teng,G. and Tuschl,T. (2004) Human Argonaute2 Mediates RNA Cleavage Targeted by miRNAs and siRNAs. *Mol. Cell*, **15**, 185–197.
7. Haley,B. and Zamore,P.D. (2004) Kinetic analysis of the RNAi enzyme complex. *Nat. Struct. Mol. Biol.*, **11**, 599–606.
8. Ma,J.B., Yuan,Y.R., Meister,G., Pei,Y., Tuschl,T. and Patel,D.J. (2005) Structural basis for 5′-end-specific recognition of guide RNA by the A. fulgidus Piwi protein. *Nature*, **434**, 666–670.
9. Martinez,J., Patkaniowska,A., Urlaub,H., Luhrmann,R. and Tuschl,T. (2002) Single-Stranded Antisense siRNAs Guide Target RNA Cleavage in RNAi. *Cell*, **110**, 563–574.

10. Leuschner Philipp,J.F., Ameres Stefan,L., Kueng,S. and Martinez,J. (2006) Cleavage of the siRNA passenger strand during RISC assembly in human cells. *EMBO Rep.*, **7**, 314–320.
11. Matranga,C., Tomari,Y., Shin,C., Bartel,D.P. and Zamore,P.D. (2005) Passenger-strand cleavage facilitates assembly of siRNA into Ago2-containing RNAi enzyme complexes. *Cell*, **123**, 607–620.
12. Rand,T.A., Petersen,S., Du,F. and Wang,X. (2005) Argonaute2 cleaves the anti-guide strand of siRNA during RISC activation. *Cell*, **123**, 621–629.
13. Allerson,C.R., Sioufi,N., Jarres,R., Prakash,T.P., Naik,N., Berdeja,A., Wanders,L., Griffey,R.H., Swayze,E.E. and Bhat,B. (2005) Fully 2′-modified oligonucleotide duplexes with improved in vitro potency and stability compared to unmodified small iInterfering RNA. *J. Med. Chem.*, **48**, 901–904.
14. Prakash,T.P., Allerson,C.R., Dande,P., Vickers,T.A., Sioufi,N., Jarres,R., Baker,B.F., Swayze,E.E., Griffey,R.H. and Bhat,B. (2005) Positional effect of chemical modifications on short interference RNA activity in Mammalian cells. *J. Med. Chem.*, **48**, 4247–4253.
15. Khvorova,A., Reynolds,A. and Jayasena,S.D. (2003) Functional siRNAs and miRNAs exhibit strand bias. *Cell*, **115**, 209–216.
16. Barker,R. and Fletcher,H.G. (1961) 2,3,5-Tri-O-benzyl-D-ribosyl and -L-arabinosyl bromides. *J. Org. Chem.*, **26**, 4605–4609.
17. Beaucage,S.L. (2008) Solid-phase synthesis of siRNA oligonucleotides. *Curr. Opin. Drug Discov. Devel.*, **11**, 203–216.
18. Mueller,S., Wolf,J. and Ivanov,S.A. (2004) Current Strategies for the Synthesis of RNA. *Curr. Org. Synth.*, **1**, 293–307.
19. Xia,J., Noronha,A., Toudjarska,I., Li,F., Akinc,A., Braich,R., Frank-Kamenetsky,M., Rajeev,K.G., Egli,M. and Manoharan,M. (2006) Gene Silencing Activity of siRNAs with a Ribo-difluorotoluyl Nucleotide. *ACS Chem. Biol.*, **1**, 176–183.
20. Schwarz,D.S., Hutvagner,G., Du,T., Xu,Z., Aronin,N. and Zamore,P.D. (2003) Asymmetry in the assembly of the RNAi enzyme complex. *Cell*, **115**, 199–208.
21. Schweitzer,B.A. and Kool,E.T. (1995) Hydrophobic, non-hydrogen-bonding bases and base pairs in DNA. *J. Am. Chem. Soc.*, **117**, 1863–1872.
22. Guckian,K.M., Schweitzer,B.A., Ren,R.X.F., Sheils,C.J., Paris,P.L. and Kool,E.T. (1996) Experimental measurement of aromatic stacking affinities in the context of duplex DNA. *J. Am. Chem. Soc.*, **118**, 8182–8183.
23. Loakes,D. and Brown,D.M. (1994) 5-Nitroindole as an universal base analogue. *Nucleic Acids Res.*, **22**, 4039–4043.
24. Li,F., Pallan,P.S., Maier,M.A., Rajeev,K.G., Mathieu,S.L., Kreutz,C., Fan,Y., Sanghvi,J., Micura,R., Rozners,E. *et al.* (2007) Crystal structure, stability and in vitro RNAi activity of oligoribonucleotides containing the ribo-difluorotoluyl nucleotide: insights into substrate requirements by the human RISC Ago2 enzyme. *Nucleic Acids Res.*, **35**, 6424–6438.
25. Somoza,A., Silverman,A.P., Miller,R.M., Chelliserrykattil,J. and Kool,E.T. (2008) Steric effects in RNA interference: probing the influence of nucleobase size and shape. *Chemistry*, **14**, 7978–7987.